

Click Synthesis, Aggregation-Induced Emission, *E*–*Z* Isomerization, Self-organization, and Multiple Chromisms of Pure Stereoisomers of a Tetraphenylethene-Cored Luminogen

Jian Wang,[†] Ju Mei,[†] Rongrong Hu,[‡] Jing Zhi Sun,^{*,†} Anjun Qin,^{*,†} and Ben Zhong Tang^{*,†,‡}

[†]MoE Key Laboratory of Macromolecular Synthesis and Functionalization, Department of Polymer Science and Engineering, Zhejiang University, Hangzhou 310027, China

[‡]Department of Chemistry, Institute for Advanced Study, Institute of Molecular Functional Materials, State Key Laboratory of Molecular Neuroscience, and Division of Biomedical Engineering, The Hong Kong University of Science & Technology, Clear Water Bay, Kowloon, Hong Kong, China

* To whom correspondence should be addressed. E-mail: sunjz@zju.edu.cn, qinag@zju.edu.cn, tangbenz@ust.hk.

Table of Contents

| | |
|--|-----|
| Measurement of Fluorescence Quantum Yield in the Solid State | (2) |
| Figure S1. The IR spectra of (a) (<i>E</i>)- and (b) (<i>Z</i>)-BPHTATPE. | (3) |
| Figure S2. ¹ H NMR spectra of (a) pure (<i>E</i>)-BPHTATPE, (b) (<i>E</i>)/(<i>Z</i>)-BPHTATPE mixture, and (c) pure (<i>Z</i>)-BPHTATPE in chloroform- <i>d</i> . The solvent peaks are marked with asterisks. | (3) |
| Figure S3. ¹³ C NMR spectra of (a) pure (<i>E</i>)-BPHTATPE, (b) (<i>E</i>)/(<i>Z</i>)-BPHTATPE mixture, and (c) pure (<i>Z</i>)-BPHTATPE in chloroform- <i>d</i> . The solvent peaks are marked with asterisks. | (4) |
| Figure S4. High resolution mass spectrum of (<i>E</i>)-BPHTATPE. | (4) |
| Figure S5. High resolution mass spectrum of (<i>Z</i>)-BPHTATPE. | (5) |
| Figure S6. Absorption spectra of (<i>E</i>)-BPHTATPE in THF/water mixtures with different fractions of water; <i>c</i> = 10 μ M. | (5) |
| Figure S7. (a) Absorption and (b) emission spectra of (<i>Z</i>)-BPHTATPE in THF/water mixtures with different fractions of water; $\lambda_{\text{ex}} = 332$ nm, <i>c</i> = 10 μ M. | (6) |
| Figure S8. Variation in the sizes of aggregates of (<i>E</i>)- and (<i>Z</i>)-isomers and an <i>E</i> / <i>Z</i> mixture (1:1) of BPHTATPE with water fractions in THF/water mixtures. | (6) |
| Figure S9. Particle size distributions of (<i>E</i>)-BPHTATPE in THF/water mixtures with water fractions of (a) 70%, (b) 80%, and (c) 90%. | (7) |
| Figure S10. Particle size distributions of (<i>Z</i>)-BPHTATPE in THF/water mixtures with water fractions of (a) 70%, (b) 80%, and (c) 90%. | (7) |
| Figure S11. Particle size distributions of an <i>E</i> / <i>Z</i> mixture (1:1) of BPHTATPE in THF/water mixtures with water fractions of (a) 70%, (b) 80%, and (c) 90%. | (7) |
| Figure S12. Time dependences of PL spectra of (<i>E</i>)-BPHTATPE in THF/water mixtures with water fractions of (a) 70%, (b) 80%, and (c) 90%; $\lambda_{\text{ex}} = 332$ nm, <i>c</i> = 10 μ M. | (8) |
| Figure S13. Time dependences of PL spectra of (<i>Z</i>)-BPHTATPE in THF/water mixtures with water fractions of (a) 70%, (b) 80%, and (c) 90%; $\lambda_{\text{ex}} = 332$ nm, <i>c</i> = 10 μ M. | (8) |
| Figure S14. Time dependences of PL spectra of an <i>E</i> / <i>Z</i> mixture (1:1) of BPHTATPE in THF/water mixtures with water fractions of (a) 70%, (b) 80%, and (c) 90%; $\lambda_{\text{ex}} = 332$ nm, <i>c</i> = 10 μ M. | (8) |

Figure S15. Variations in the solid-state quantum yields of (a) (*E*)- and (b) (*Z*)-BPHTATPE with time. (9)

Figure S16. (a) Absorption and (b) emission spectra of an *E/Z* mixture (1:1) of BPHTATPE in THF/water mixtures with different fractions of water; $\lambda_{\text{ex}} = 332$ nm, $c = 10 \mu\text{M}$. (9)

Figure S17. Variation in the quantum yield (Φ_F) of an *E/Z* mixture (1:1) of BPHTATPE with water fractions in THF/water mixtures. Φ_F values estimated using quinine sulfate in 0.05 mol/L H_2SO_4 ($\Phi_F = 54.6\%$) as standard. Inset: fluorescent images of the solution in THF and the suspensions in THF/water mixtures ($f_w = 60\text{--}90\%$). (10)

Table 1. Photo^a- and thermo^b-induced *E*-*Z* isomerizations of (*E*)-BPHTATPE (10)

Figure S18. ^1H NMR spectra of (*E*)-BPHTATPE exposed to UV lamp (365 nm) for (a) 2, (b) 6, (c) 11, (d) 20, (e) 30, and (f) 50 min in CDCl_3 . Insets: enlarged spectra. P_Z : peaks for *Z*-conformer. (11)

Figure S19. ^1H NMR spectra of (a) pure (*E*)-BPHTATPE and its solutions in CDCl_3 exposed to a UV lamp (365 nm) for (b) 70, (c) 90, (d) 120, and (e) 150 min, and (f) pure (*Z*)-BPHTATPE. Insets: enlarged spectra. P_Z : peaks for *Z*-conformer. (12)

Figure S20. TGA thermograms of (*E*)- and (*Z*)-BPHTATPE recorded under nitrogen at a heating rate of 20 $^{\circ}\text{C}/\text{min}$. (13)

Figure S21. ^1H NMR spectra of (a) (*E*)-BPHTATPE heated at 180 $^{\circ}\text{C}$ and (b) (*Z*)-BPHTATPE heated at 165 $^{\circ}\text{C}$ for 30 min. (13)

Figure S22. ^1H NMR spectra of (*E*)-BPHTATPE heated at 203 $^{\circ}\text{C}$ for (a) 5, (b) 10, (c) 20, (d) 30, (e) 45, (f) 60, (g) 90, (h) 120, and (i) 150 min in chloroform-*d*. Insets: enlarged spectra. P_Z : peaks for *Z*-conformer. (14)

Figure S23. ^1H NMR spectra of (a, b) (*E*)- and (c) (*Z*)-BPHTATPE irradiated by the excitation light in a spectrofluorometer for 30 min with a wavelength of (a, c) 332 or (b) 254 nm. Insets: enlarged spectra. (15)

Figure S24. PL spectra of ground (*E*)-BPHTATPE heated at (a) 100, (b) 110, (c) 120, (d) 140 and (e) 160 $^{\circ}\text{C}$ for different time; $\lambda_{\text{ex}} = 332$ nm. (15)

Figure S25. Mechanochromic processes of (*E*)/(*Z*)-BPHTATPE mixtures with mole ratios of (a) 8:2, (c) 5:5, and (e) 2:8. G and H represent the procedures of grinding and heating at 120 $^{\circ}\text{C}$ for 1 min. The corresponding PL spectra of the mixtures after grinding and then heating at 120 $^{\circ}\text{C}$ for 1 min are shown in panels (b), (d) and (f). (16)

Figure S26. PL spectra of (*E*)-BPHTATPE before and after pressing; $\lambda_{\text{ex}} = 332$ nm. (16)

Measurement of Fluorescence Quantum Yield in the Solid State. The Φ_F values of *E* and *Z* isomers of BPHTATPE were measured with a calibrated integrating sphere on a time-resolved fluorescence spectroscopy, using eq 1 given below:¹

$$\Phi_F = \frac{N_{\text{em}}}{N_{\text{ab}}} = \frac{\alpha \int \frac{\lambda}{hc} I_{\text{em}}(\lambda) d\lambda}{\alpha \int \frac{\lambda}{hc} [I_{\text{ex}}(\lambda) - I'_{\text{ex}}(\lambda)] d\lambda} \quad (1)$$

where N_{em} and N_{ab} are the numbers of emitted and absorbed photons, respectively, α is the calibration factor for the measurement setup, λ is the wavelength, h is the Plank's constant, c is the speed of light, $I_{\text{em}}(\lambda)$ is the emission intensity at λ , and $I_{\text{ex}}(\lambda)$ and $I'_{\text{ex}}(\lambda)$ are the intensities of the excitation laser beam with λ in the absence and presence of the sample, respectively. The measured Φ_F value is independent of sharp and thickness of sample and power of excitation laser.

(1) Kawamura, Y.; Sasabe, H.; Adachi, C. *Jpn. J. Appl. Phys.* **2004**, *43*, 7729–7730.

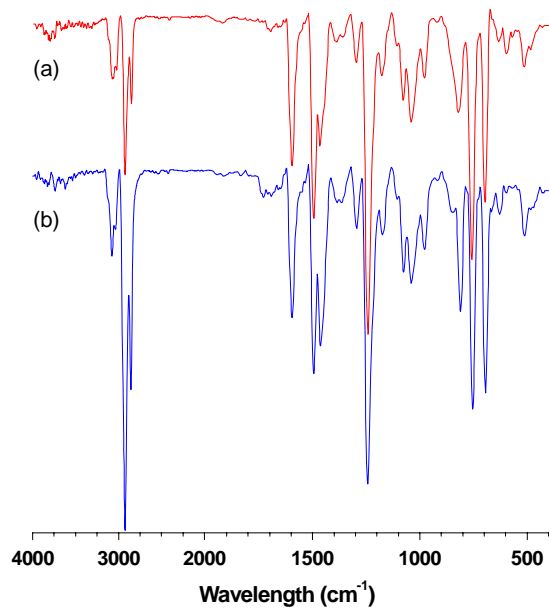


Figure S1. The IR spectra of (a) (*E*)- and (b) (*Z*)-BPHTATPE.

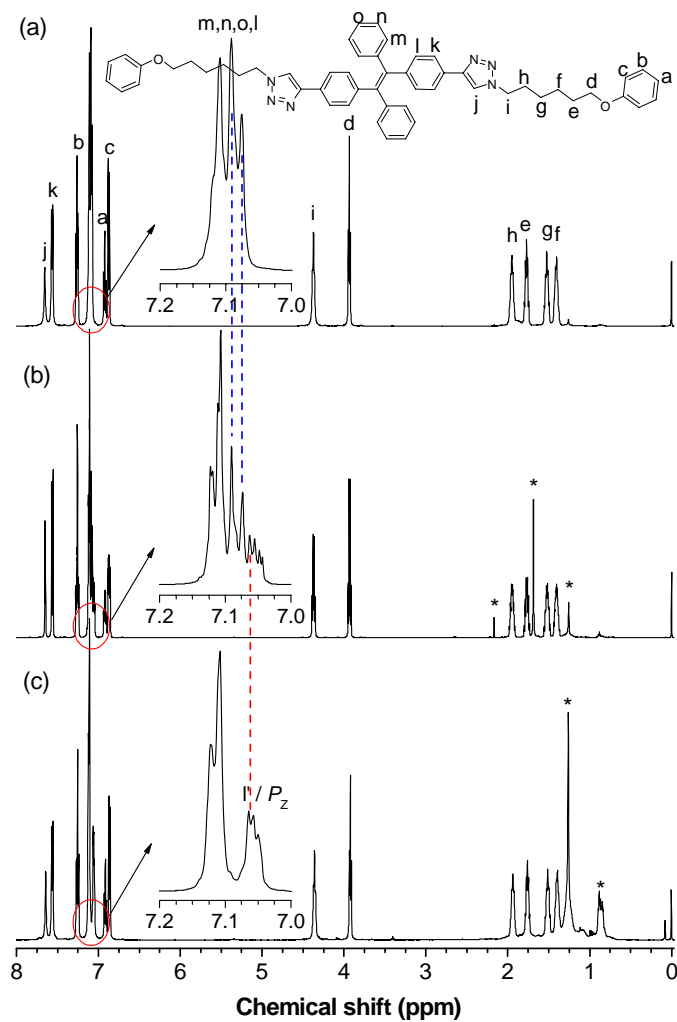


Figure S2. ^1H NMR spectra of (a) pure (*E*)-BPHTATPE, (b) (*E*)/(*Z*)-BPHTATPE mixture, and (c) pure (*Z*)-BPHTATPE in chloroform-*d*. The solvent peaks are marked with asterisks.

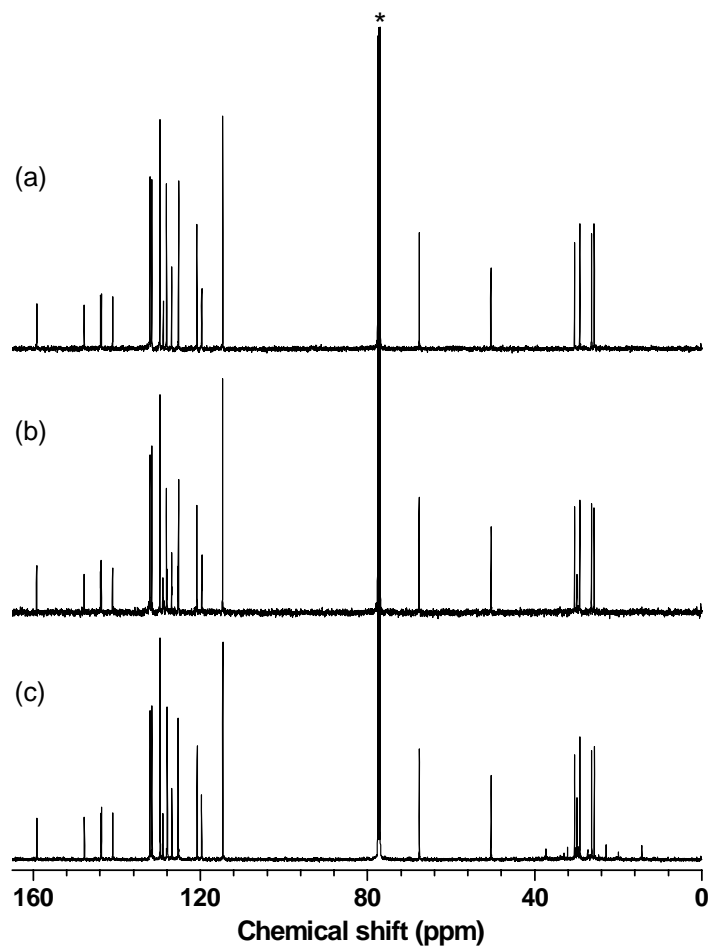


Figure S3. ^{13}C NMR spectra of (a) pure (*E*)-BPHTATPE, (b) (*E*)/(*Z*)-BPHTATPE mixture, and (c) pure (*Z*)-BPHTATPE in chloroform-*d*. The solvent peaks are marked with asterisks.

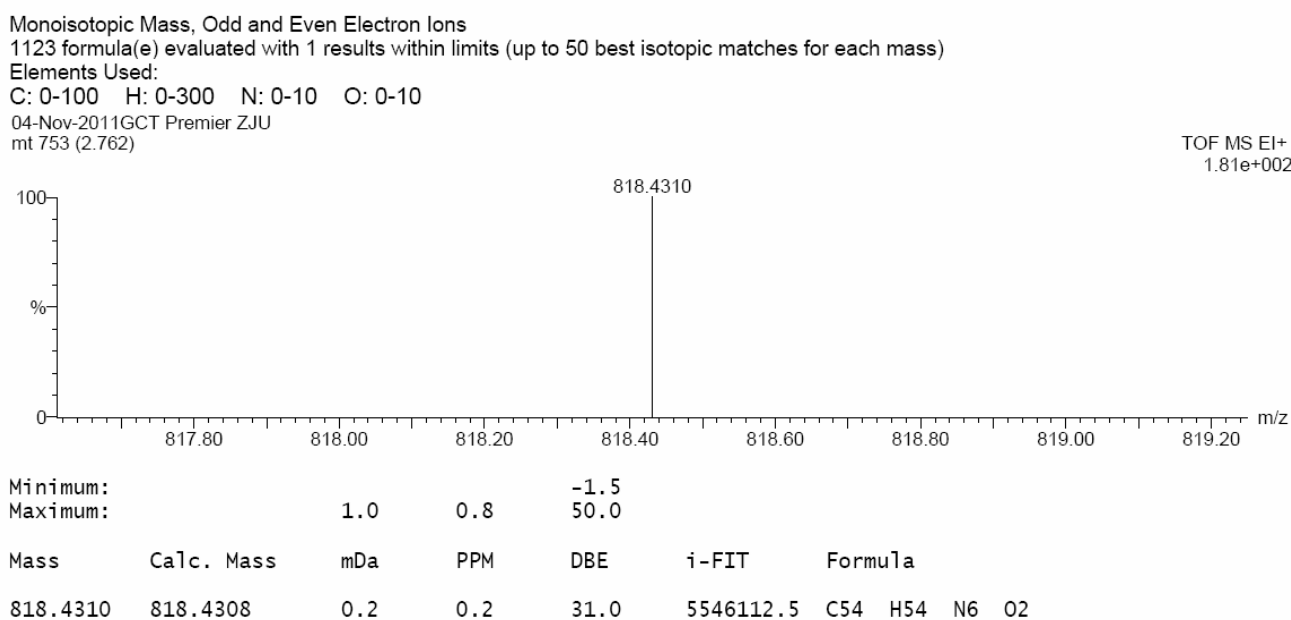
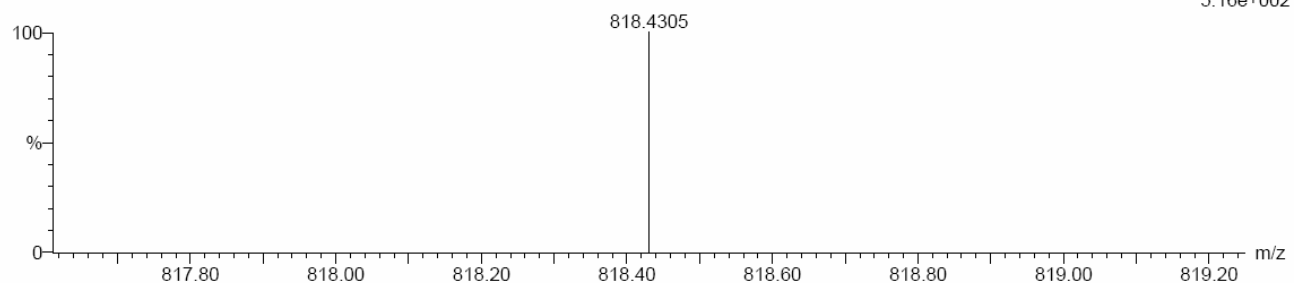


Figure S4. High resolution mass spectrum of (*E*)-BPHTATPE.

Monoisotopic Mass, Odd and Even Electron Ions
 1123 formula(e) evaluated with 1 results within limits (up to 50 best isotopic matches for each mass)
 Elements Used:
 C: 0-100 H: 0-300 N: 0-10 O: 0-10
 04-Nov-2011GCT Premier ZJU
 mc 923 (3.385)

TOF MS EI+
 5.16e+002



| | | | | | | |
|----------|------------|------|------|------|-----------|---------------|
| Minimum: | 1.0 | 0.8 | -1.5 | | | |
| Maximum: | | | 50.0 | | | |
| Mass | Calc. Mass | mDa | PPM | DBE | i-FIT | Formula |
| 818.4305 | 818.4308 | -0.3 | -0.4 | 31.0 | 5546280.0 | C54 H54 N6 O2 |

Figure S5. High resolution mass spectrum of (Z)-BPHTATPE.

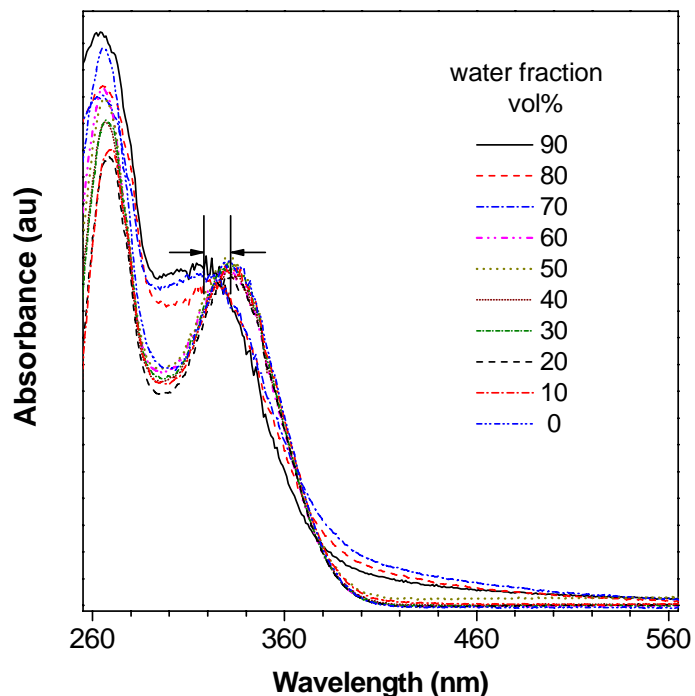


Figure S6. Absorption spectra of (E)-BPHTATPE in THF/water mixtures with different fractions of water; $c = 10 \mu\text{M}$.

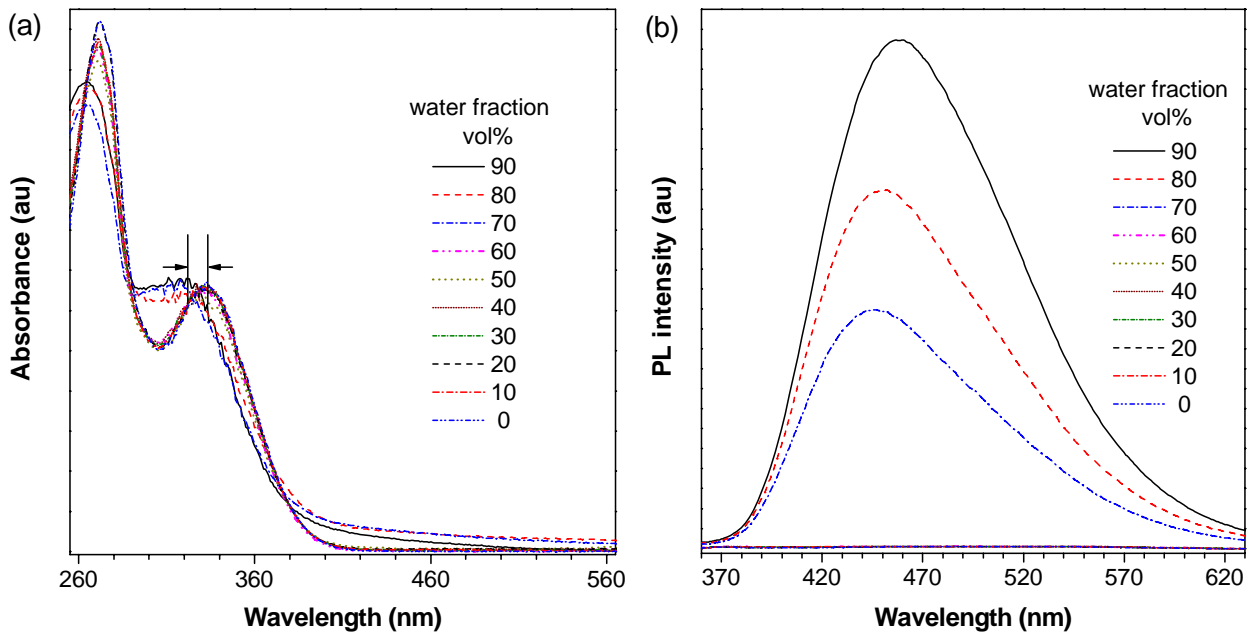


Figure S7. (a) Absorption and (b) emission spectra of (Z)-BPHTATPE in THF/water mixtures with different fractions of water; $\lambda_{\text{ex}} = 332$ nm, $c = 10 \mu\text{M}$.

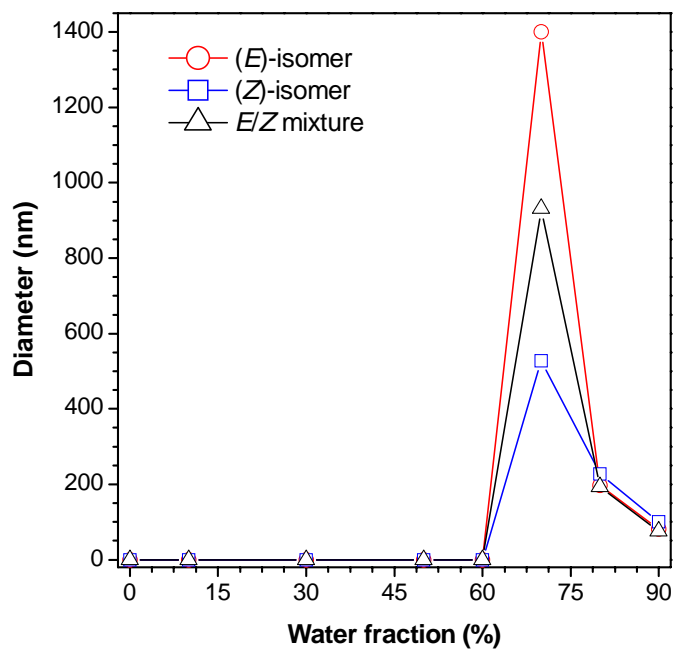


Figure S8. Variation in the sizes of aggregates of (E)- and (Z)-isomers and an E/Z mixture (1:1) of BPHTATPE with water fractions in THF/water mixtures.

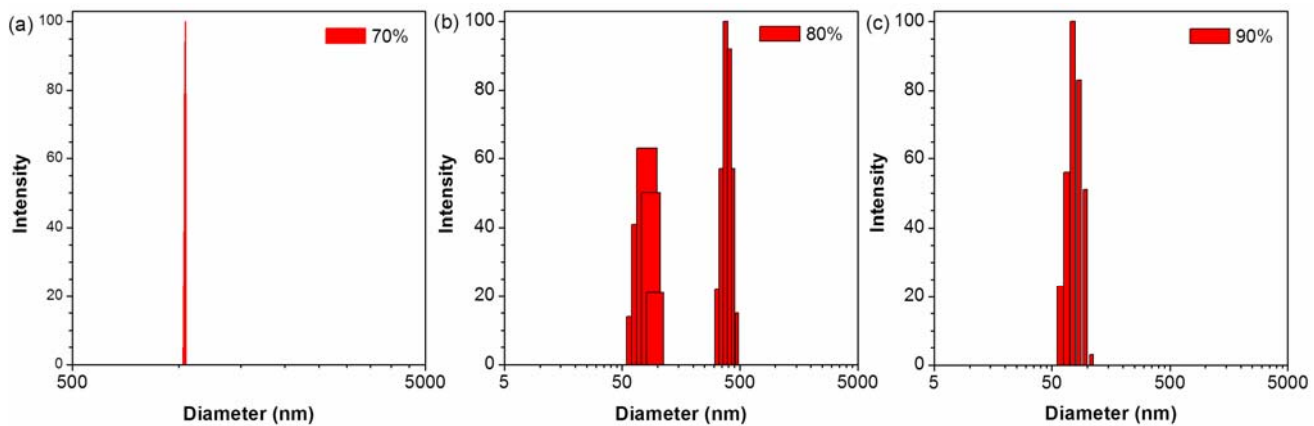


Figure S9. Particle size distributions of (E)-BPHTATPE in THF/water mixtures with water fractions of (a) 70%, (b) 80%, and (c) 90%.

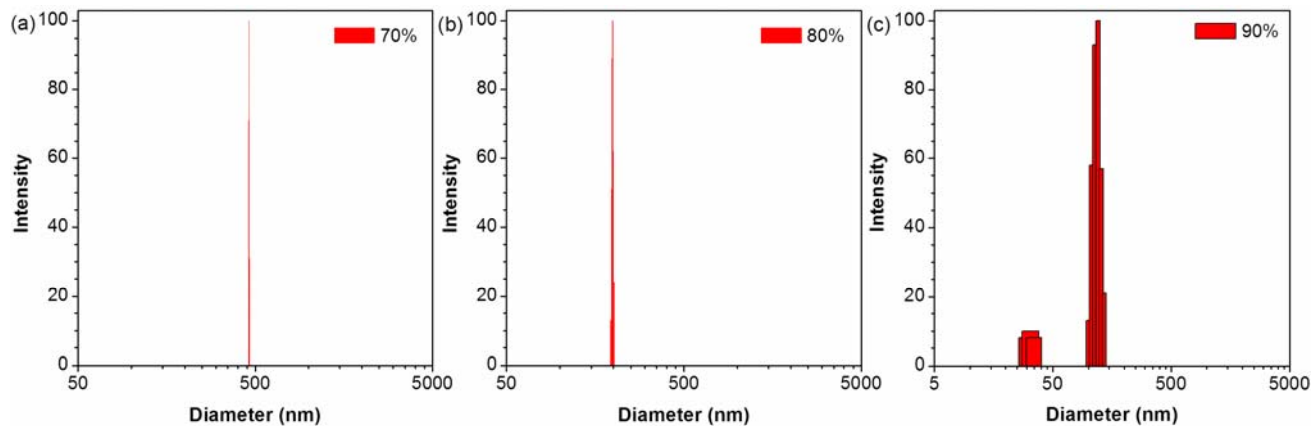


Figure S10. Particle size distributions of (Z)-BPHTATPE in THF/water mixtures with water fractions of (a) 70%, (b) 80%, and (c) 90%.

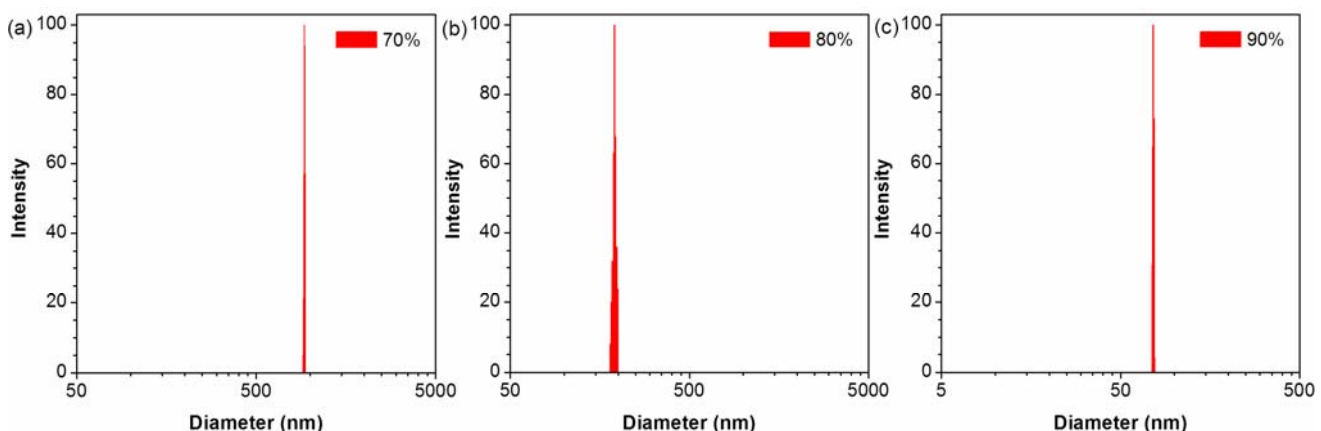


Figure S11. Particle size distributions of an E/Z mixture (1:1) of BPHTATPE in THF/water mixtures with water fractions of (a) 70%, (b) 80%, and (c) 90%.

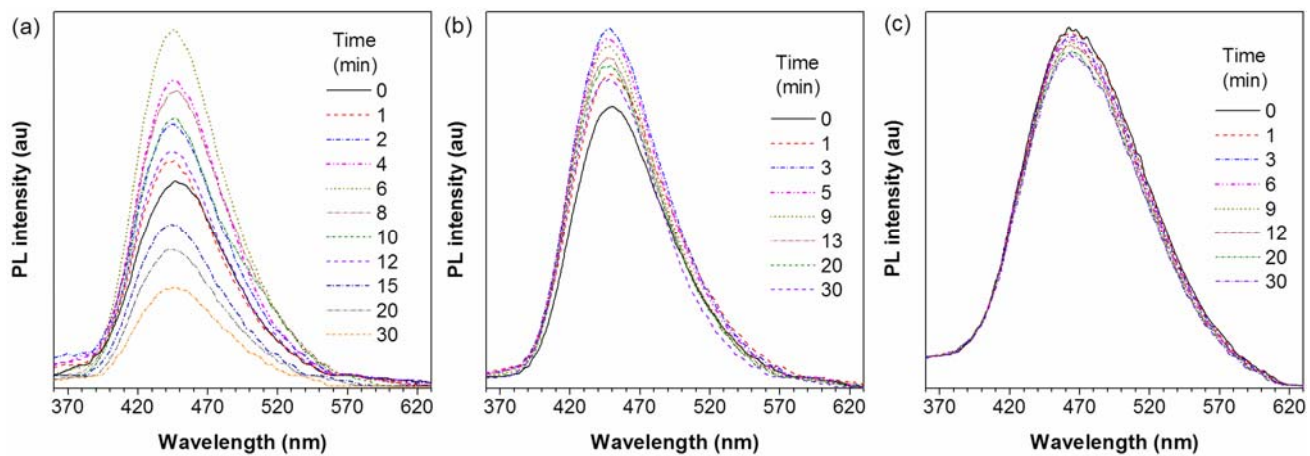


Figure S12. Time dependences of PL spectra of (*E*)-BPHTATPE in THF/water mixtures with water fractions of (a) 70%, (b) 80%, and (c) 90%; $\lambda_{\text{ex}} = 332$ nm, $c = 10$ μM .

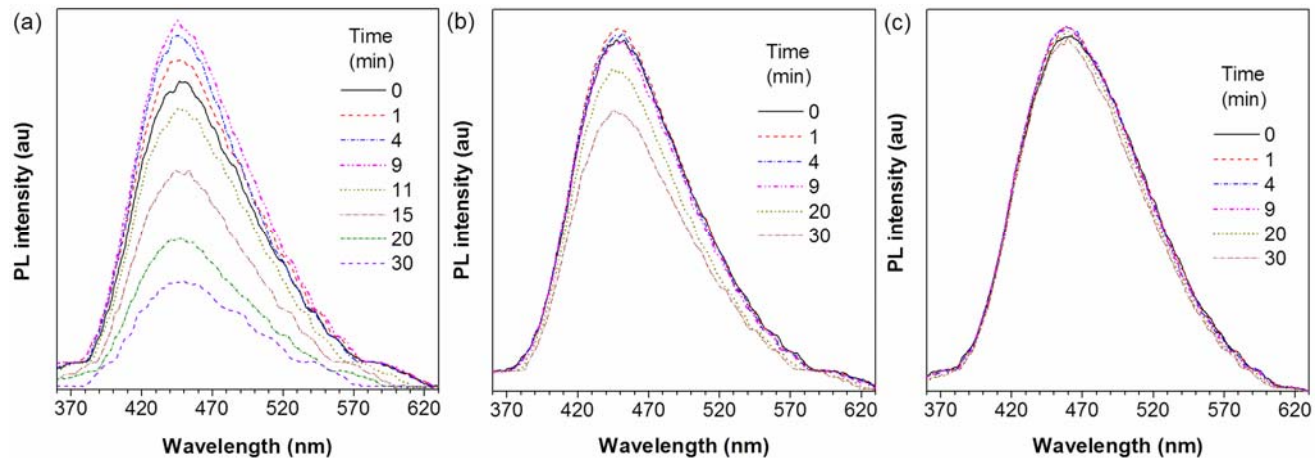


Figure S13. Time dependences of PL spectra of (*Z*)-BPHTATPE in THF/water mixtures with water fractions of (a) 70%, (b) 80%, and (c) 90%; $\lambda_{\text{ex}} = 332$ nm, $c = 10$ μM .

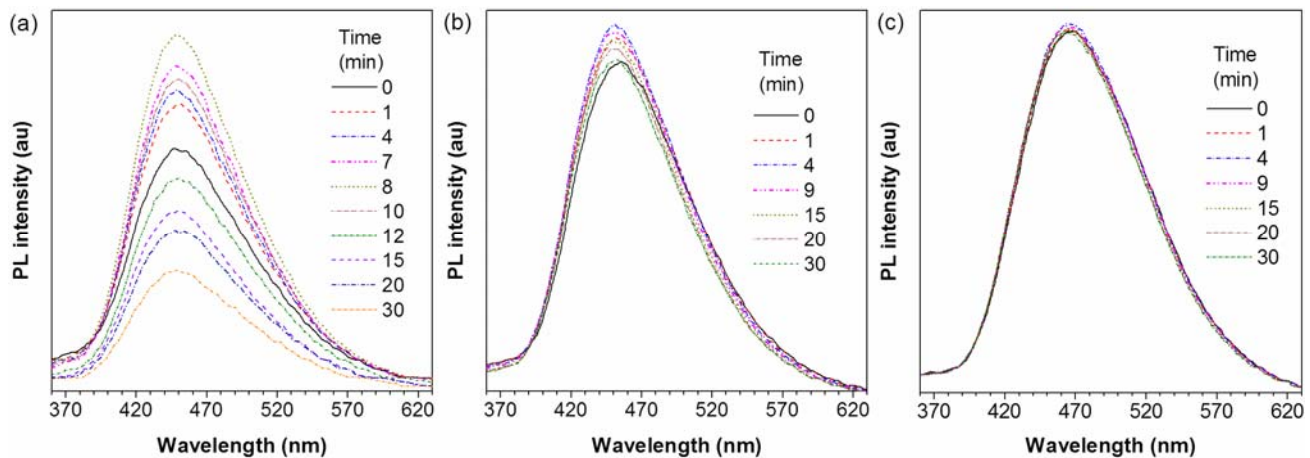


Figure S14. Time dependences of PL spectra of an *E/Z* mixture (1:1) of BPHTATPE in THF/water mixtures with water fractions of (a) 70%, (b) 80%, and (c) 90%; $\lambda_{\text{ex}} = 332$ nm, $c = 10$ μM .

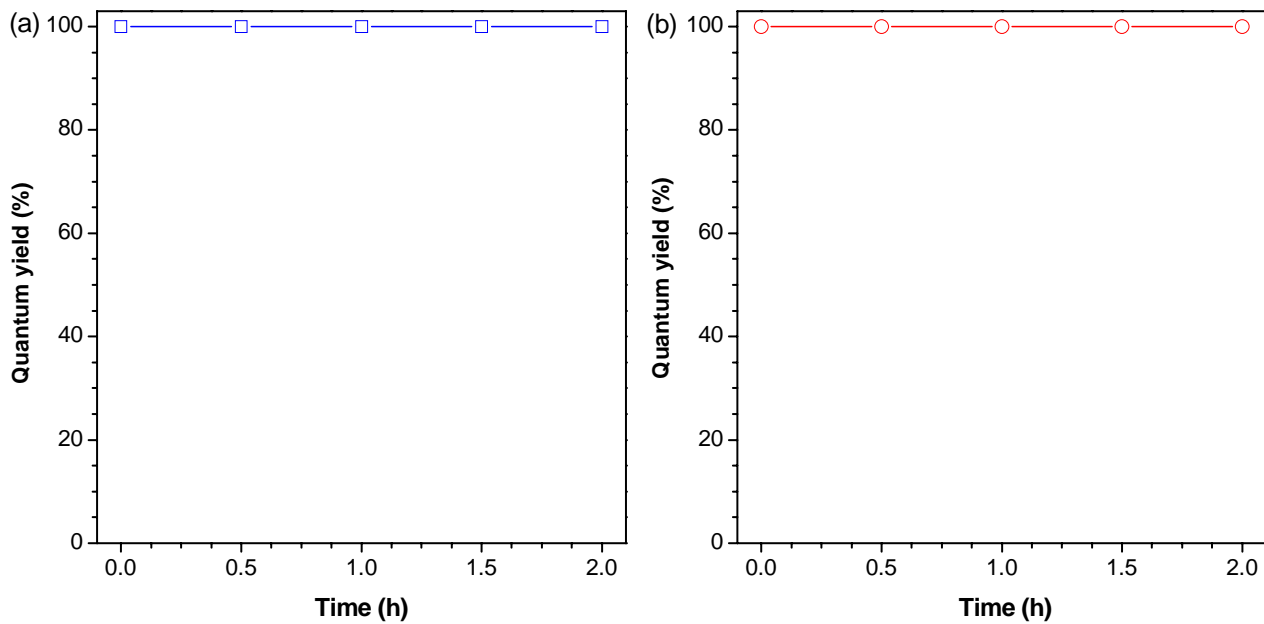


Figure S15. Variations in the solid-state quantum yields of (a) (*E*)- and (b) (*Z*)-BPHTATPE with time.

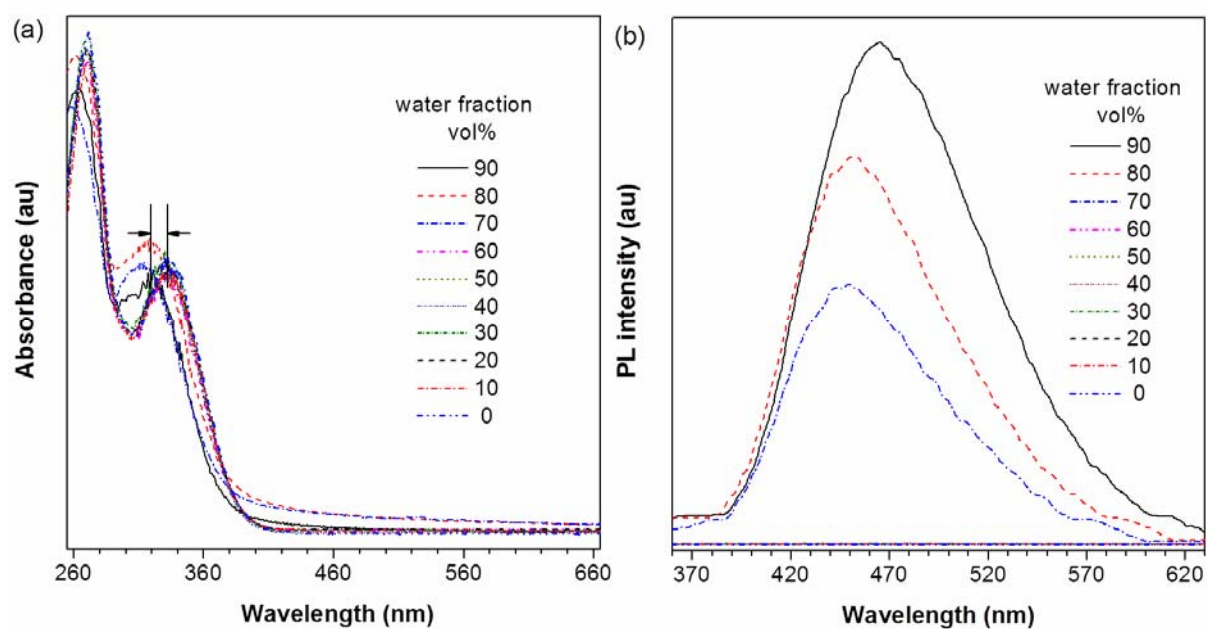


Figure S16. (a) Absorption and (b) emission spectra of an *E/Z* mixture (1:1) of BPHTATPE in THF/water mixtures with different fractions of water; $\lambda_{\text{ex}} = 332$ nm, $c = 10$ μM .

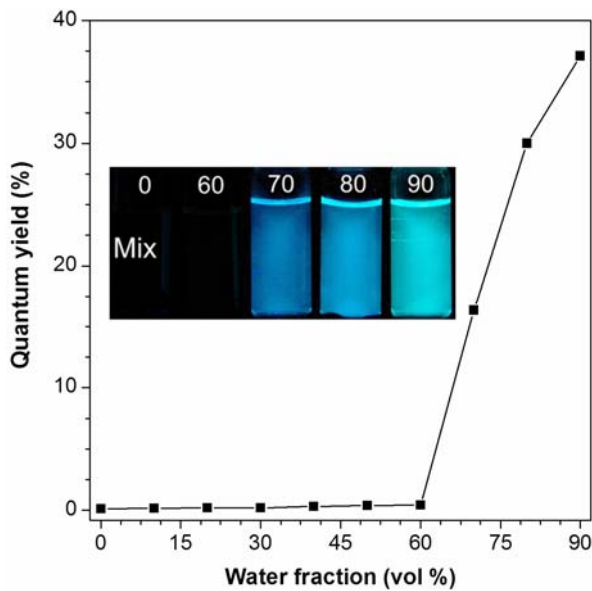


Figure S17. Variation in the quantum yield (Φ_F) of an *E*/*Z* mixture (1:1) of BPHTATPE with water fractions in THF/water mixtures. Φ_F values estimated using quinine sulfate in 0.05 mol/L H_2SO_4 ($\Phi_F = 54.6\%$) as standard. Inset: fluorescent images of the solution in THF and the suspensions in THF/water mixtures ($f_w = 60\text{--}90\%$).

Table S1. Photo^a- and thermo^b-induced *E*-*Z* isomerizations of (*E*)-BPHTATPE

| no. | time (min) | integral quantity of peak <i>Z</i> ^b | <i>f_Z</i> (%) ^c | |
|---------------------|------------|---|---------------------------------------|------------------------------|
| | | | (from peak <i>Z</i>) ^c | (from triazole) ^d |
| photoisomerization | | | | |
| 1 | 2 | 0.04 | 1.0 | |
| 2 | 6 | 0.16 | 4.0 | |
| 3 | 11 | 0.28 | 7.0 | |
| 4 | 20 | 0.58 | 14.5 | |
| 5 | 30 | 1.00 | 25.0 | |
| 6 | 50 | 1.40 | 35.0 | 35.1 |
| 7 | 70 | 1.68 | 42.0 | 41.8 |
| 8 | 90 | 1.80 | 45.0 | 44.3 |
| 9 | 120 | 1.94 | 48.5 | 47.9 |
| 10 | 150 | 2.02 | 50.5 | 50.3 |
| thermoisomerization | | | | |
| 11 | 5 | 0.12 | 3.0 | |
| 12 | 10 | 0.24 | 6.0 | |
| 13 | 20 | 0.40 | 10.0 | |
| 14 | 30 | 0.56 | 14.0 | |
| 15 | 45 | 1.00 | 25.0 | |
| 16 | 60 | 1.38 | 34.5 | 34.7 |
| 17 | 90 | 1.76 | 44.0 | 43.5 |
| 18 | 120 | 1.86 | 46.5 | 46.1 |
| 19 | 150 | 1.92 | 48.0 | 47.5 |

^a For photoisomerization, solutions of (*E*)-BPHTATPE in chloroform-*d* were exposed to a UV light of 365 nm at room temperature; for thermoisomerization, powders of (*E*)-BPHTATPE were heated to 203 °C under nitrogen. ^b Set the integral quantity of the peaks lying between 7.2 and 7.0 ppm in ¹H NMR as 14 when quantifying the quantity of peak *Z*. ^c Fraction of *Z*-conformer calculated from peak *Z*. ^d Fraction of *Z*-conformer calculated by fitting the two peaks corresponding to the hydrogen of triazole groups of *E* (7.654 ppm) and *Z* (7.645 ppm) isomers.

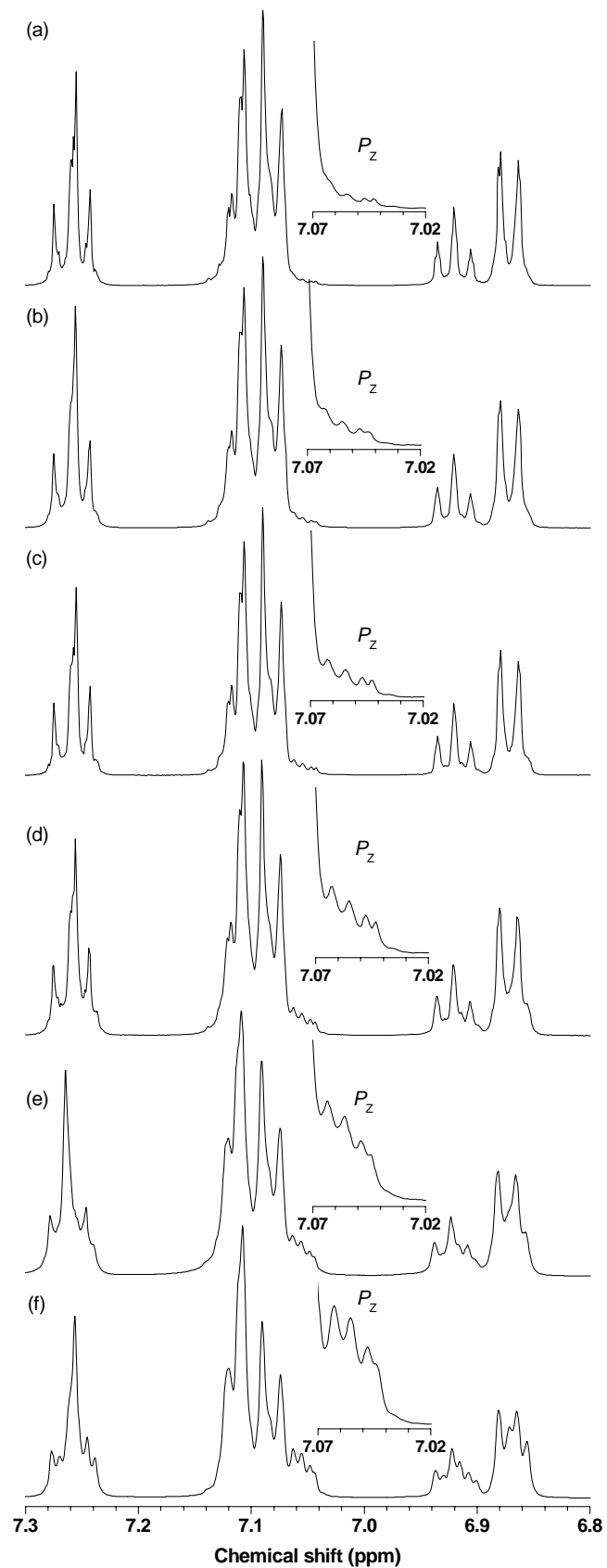


Figure S18. ^1H NMR spectra of (E)-BPHTATPE exposed to UV lamp (365 nm) for (a) 2, (b) 6, (c) 11, (d) 20, (e) 30, and (f) 50 min in CDCl_3 . Insets: enlarged spectra. P_Z : peaks for Z-conformer.

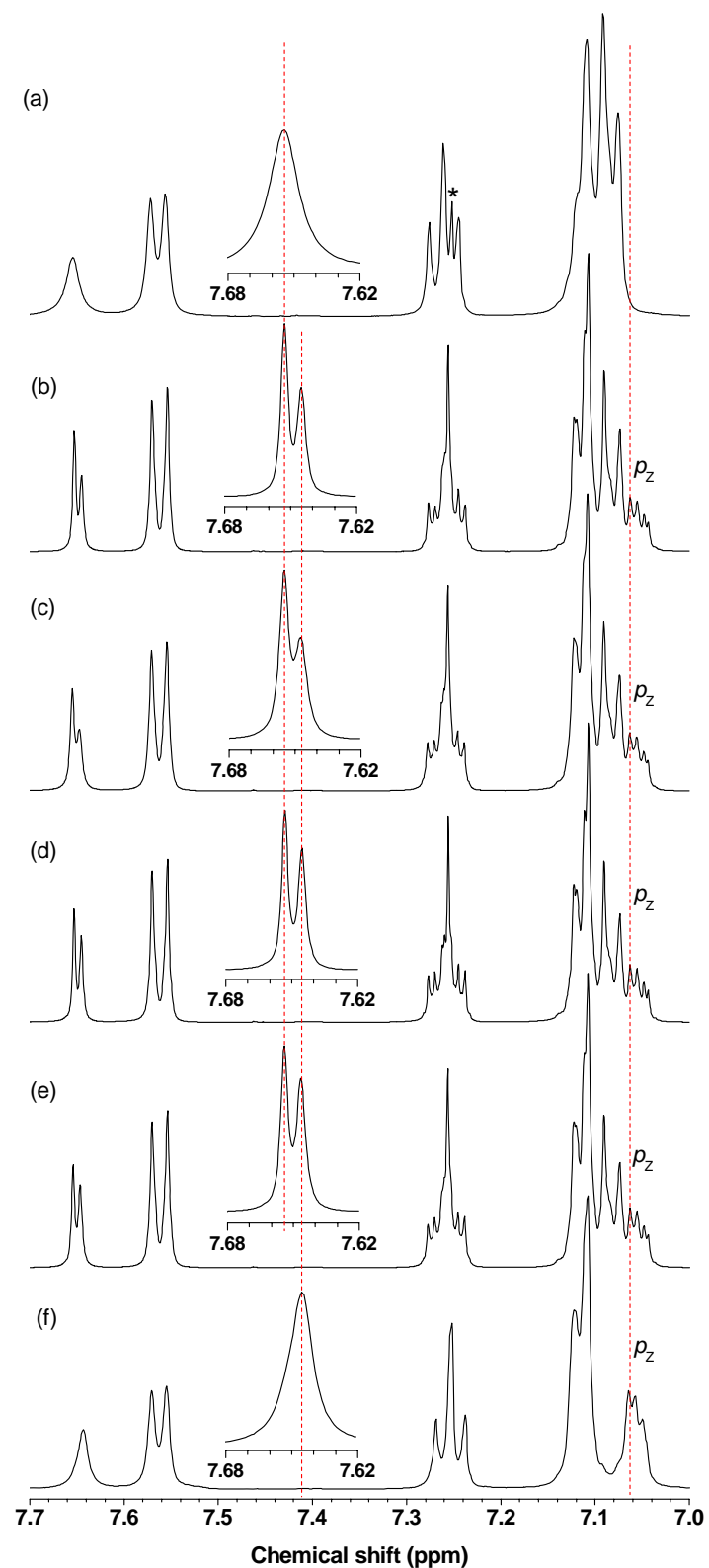


Figure S19. ^1H NMR spectra of (a) pure (*E*)-BPHTATPE and its solutions in CDCl_3 exposed to a UV lamp (365 nm) for (b) 70, (c) 90, (d) 120, and (e) 150 min, and (f) pure (*Z*)-BPHTATPE. Insets: enlarged spectra. P_z : peaks for *Z*-conformer.

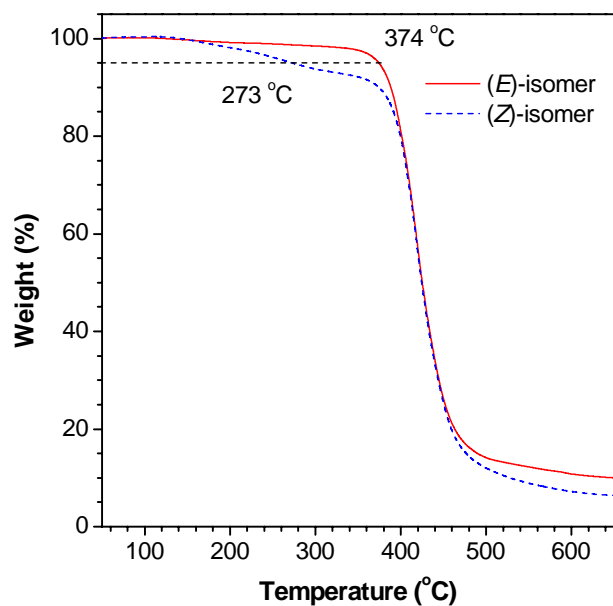


Figure S20. TGA thermograms of (*E*)- and (*Z*)-BPHTATPE recorded under nitrogen at a heating rate of 20 °C/min.

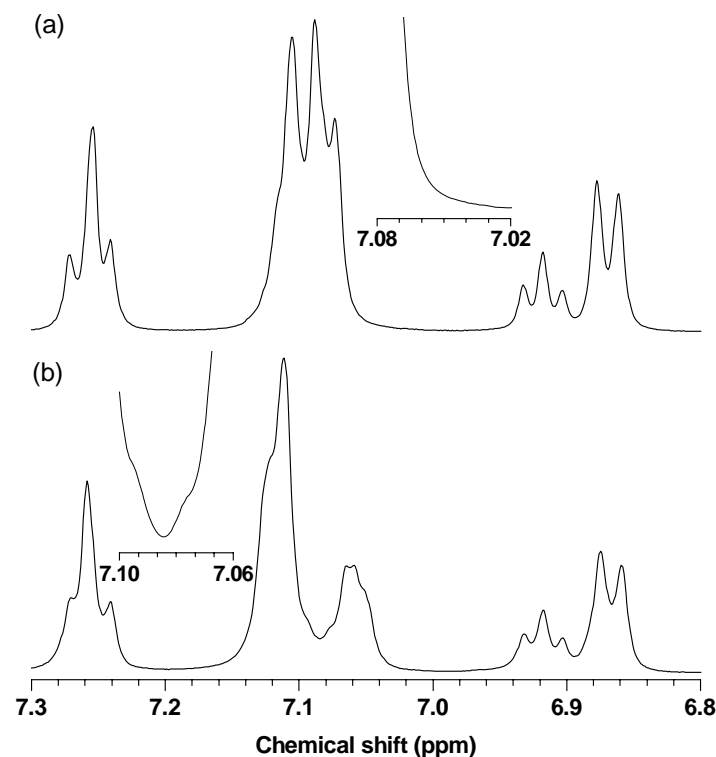


Figure S21. ^1H NMR spectra of (a) (*E*)-BPHTATPE heated at 180 °C and (b) (*Z*)-BPHTATPE heated at 165 °C for 30 min.

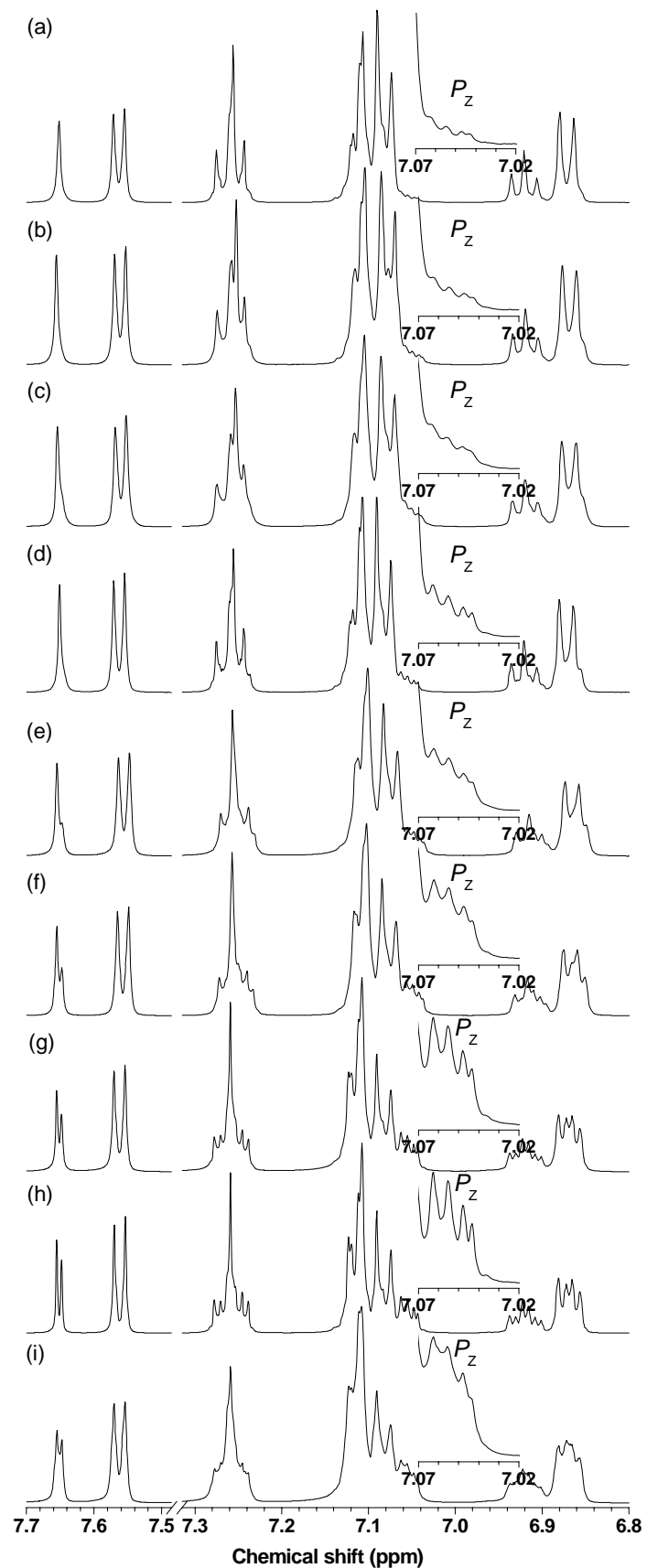


Figure S22. ^1H NMR spectra of (E)-BPHTATPE heated at 203 °C for (a) 5, (b) 10, (c) 20, (d) 30, (e) 45, (f) 60, (g) 90, (h) 120, and (i) 150 min in chloroform- d . Insets: enlarged spectra. P_z : peaks for Z-conformer.

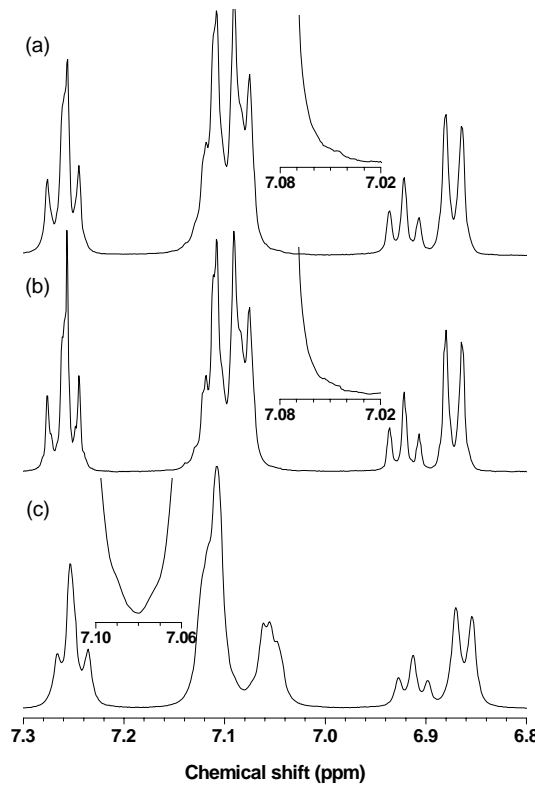


Figure S23. ^1H NMR spectra of (a, b) (*E*)- and (c) (*Z*)-BPHTATPE irradiated by the excitation light in a spectrofluorometer for 30 min with a wavelength of (a, c) 332 or (b) 254 nm. Insets: enlarged spectra.

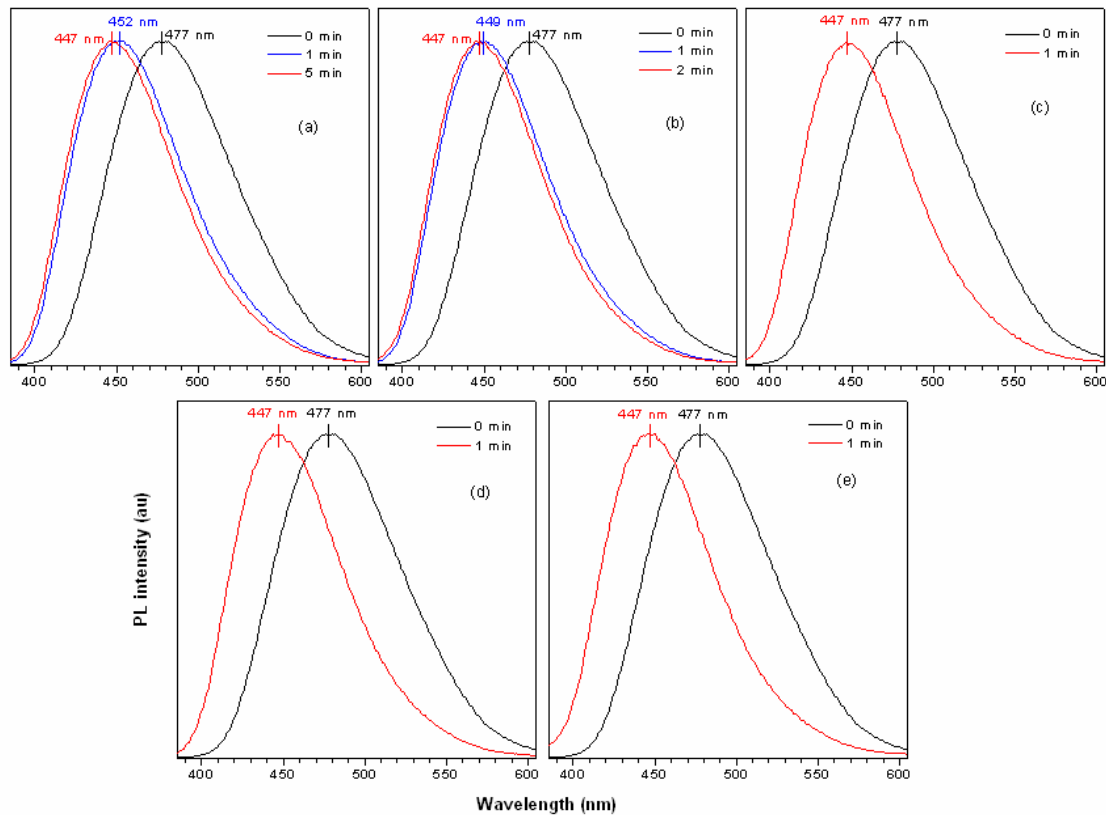


Figure S24. PL spectra of ground (*E*)-BPHTATPE heated at (a) 100, (b) 110, (c) 120, (d) 140 and (e) 160 $^{\circ}\text{C}$ for different time; $\lambda_{\text{ex}} = 332$ nm.

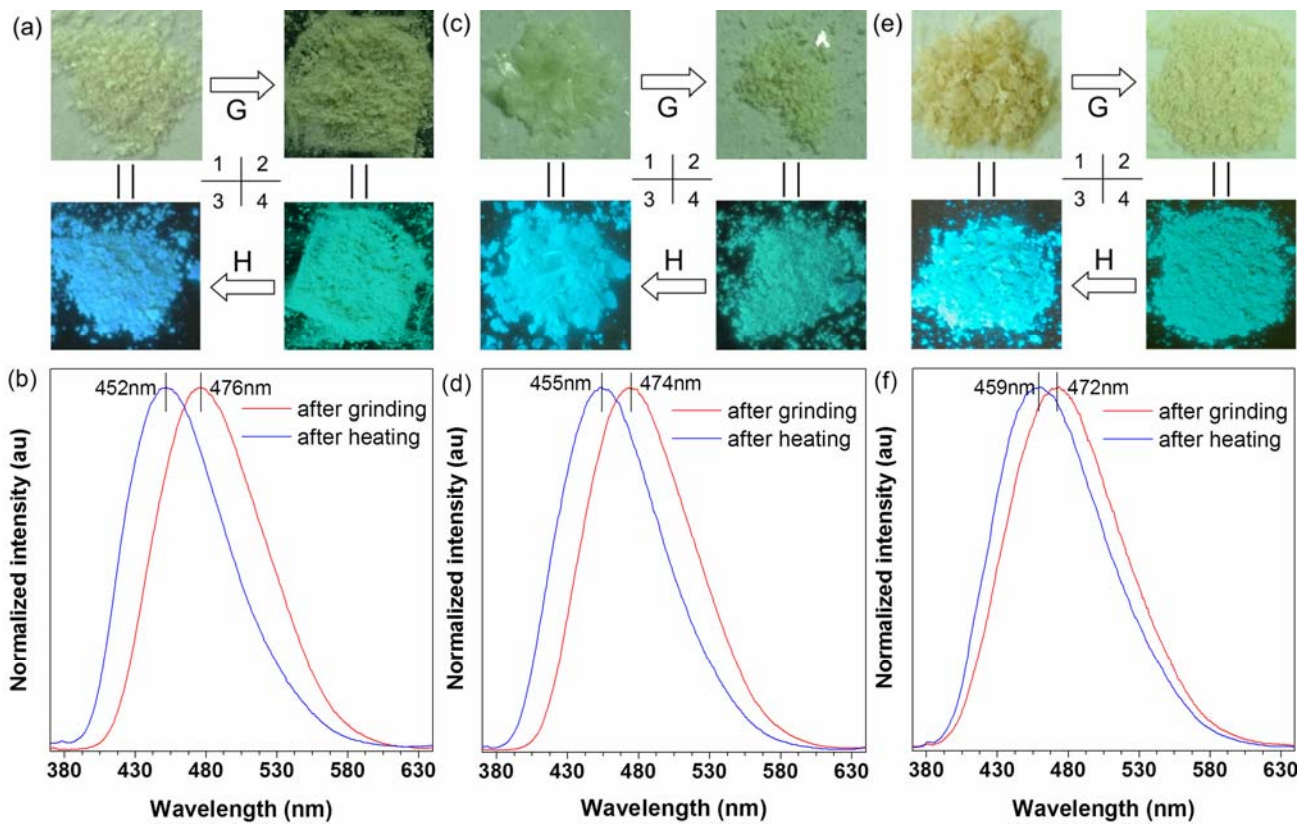


Figure S25. Mechanochromic processes of (E)/(Z)-BPHTATPE mixtures with mole ratios of (a) 8:2, (c) 5:5, and (e) 2:8. G and H represent the procedures of grinding and heating at 120 °C for 1 min. The corresponding PL spectra of the mixtures after grinding and then heating at 120 °C for 1 min are shown in panels (b), (d) and (f).

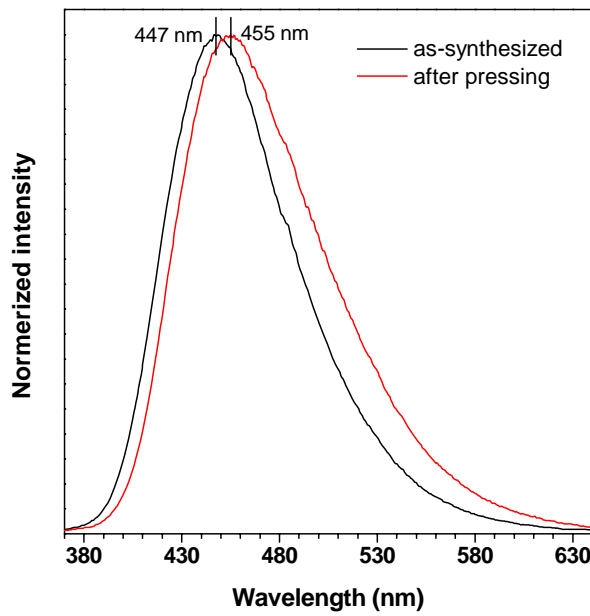


Figure S26. PL spectra of (E)-BPHTATPE before and after pressing; $\lambda_{\text{ex}} = 332$ nm.